Proc. Natl. Sci. Counc. ROC(A)
Vol. 23, No. 1, 1999. pp. 20-30

Wire-Frame Method for Blending Surface Design

DAH-JYH GUAN*, ZI-CAI LI*, YAN-LIANG CHEN*, AND JUNG-HONG CHUANG**

**Department of Applied Mathematics*
National Sun Yat-Sen University
Kaohsiung, Taiwan , R.O.C.
***Department of Computer and Information Engineering*
National Chiao-Tung University
Hsinchu, Taiwan, R.O.C.

(Received February 23, 1998; Accepted May 18, 1998)

ABSTRACT

This paper introduces a wire-frame method for the generation of blending surfaces. It is a numerical approach to the design of surfaces that smoothly join two or more given surfaces. The blending surface generated by the wire-frame method is composed of a set of bicubic patches in parametric forms. The wire-frame method first constructs a set of wire-frames. Each element of the wire-frame is modeled as an elastic beam subject to external load. The stiffness of the beam and the distribution of the load are used to control the shape of the blending surfaces. The shape of the wire-frames can then be computed from the deflection of the beams. After the wire-frame is constructed, a set of bicubic patch can then be computed from the interpolating polynomials using the tensor product rule.

Key Words: computer aided geometric design, blending surface, parametric form, bicubic patch, ordinary differential equation, numerical solution, finite element method

I. Introduction

A blending surface is a surface that smoothly joins two or more given surfaces. In computer aided geometry design, solid objects are often represented by their boundary surfaces. These boundary surfaces can be classified into two types: *primary surfaces* and *blending surfaces*. In most cases, the shape of an object is mainly defined by the primary surfaces. However, blending surfaces in geometry design are important because sharp edges and corners are undesirable for functional or aesthetic reasons. Therefore, it is desirable to generate a blending surface automatically from the given primary surfaces so that the resulting surfaces not only meet the aesthetic or safety requirements, but also reduce the stress concentration and turbulence flow. Automatic generation of blending surfaces can help designers to design blending surfaces which are usually more complex in mathematical representation. Thus, designers can concentrate on the design of primary surfaces.

In this paper, we propose a *wire-frame* method for the generation of blending surfaces. It is a numerical approach to the design of blending surfaces. The blending surface generated using the wire-frame method is composed of a set of bicubic patches with wire-frames as the boundaries of each patch.

Surfaces in R^3 can be represented either *algebraically* or *parametrically*. Both representations are widely used in computer aided geometry design. Blending surfaces generated by the wire-frame method are represented in parametric form.

The wire-frame method first constructs a set of wire-frames. The wire frames are modeled by fourth-order ordinary differential equations with boundary conditions. The differential equations are then solved using the finite element method. After the wire frames are constructed, a set of bicubic patches can be computed through interpolation.

We distinguish two types of wire frames. Wire frames that connect the primary surfaces are called *latitudinal* wire frames, and wire frames along the other coordinate are called *longitudinal* wire frames. In the construction of wire-frames, each element of the wire-frame is modeled as an elastic beam subject to an external load. The shape of the wire-frame can then be computed from the deflection of the beam under the external load. After the wire frames are constructed, the boundaries of each bicubic patch are known, and a set of bicubic patches can then be computed from the interpolating polynomials using the tensor product rule.

The blending surface is governed by a set of fourth-order ordinary differential equations that describe the deflections of the elastic beam. The stiffness

of the beam and the distribution of the load can be used to control the shape of the blending surfaces.

Our results compare with those of others as follows. Most of the researches on blending surfaces have been done with algebraic surfaces, for example, those of Hoffmann and Hopcroft (1985, 1986, 1987, 1988), Kosters (1989), Ohkura and Kakazu (1992), Warren (1987, 1989), Bajaj and Ihm (1992), and Holmström (1987). For parametric surfaces, Vida, Martin, and Varady provided a comprehensive review of solutions that use parametric surfaces (Vida *et al*., 1994).

Blending can also be regarded as interpolation. However, blending differs from interpolation in that interpolation needs to satisfy more conditions, for example, passing a set of given points. Blending, in general, does not need such restrictions. We may develop a general equation to model blending so that a set of blending surfaces can be generated. Interpolation was used by Lounsbery *et al*. (1992) and Filip (1989). Interpolation with minimizing energy function or some form of norms has been used by Nielson (1980, 1983), Kallay and Ravani (1990), Celniker and Gossard (1991), and Moreton and Séquin (1992). Bloor and Wilson presented methods using partial differential equations to generate blending surfaces (Bloor and Wilson, 1989, 1990a, 1990b).

The algebraic degree of the surfaces is crucial for manipulation of the objects they represent. For example, the computational time needed to display and to do intersection, union and other operations on the solid objects depends crucially on the algebraic degree of the surfaces. Therefore, only low-degree surfaces are used in most of the computer aided design systems. Since a blending surface should be tangent to two or more primary surfaces, it has, in general, a higher degree than either of the surfaces it joins. It has been shown that if the intersection of the two primary surfaces is a single quartic space curve, then any blending surface must be of at least degree four (Hoffmann and Hopcroft, 1986; Warren, 1987, 1989). The blending surface generated using the wire-frame method is a set of bicubic patches. Most of the existing computer aided geometry design tools can handle further operations on the surfaces generated using our method.

This paper is organized as follows. We first develop differential equations that can be used to generate blending surfaces. We then show how to solve the latitudinal wire frame extending from one primary surface to the other primary surface. Since the transfer points are now known, the longitudinal wire frame can also be obtained by solving a similar fourth-order differential equation. The bicubic patches of the blending surface can then be obtained using the tensor-product rule. In addition to the theoretical work, we also give examples to demonstrate the effectiveness of our wire-frame method in the design of blending surfaces. Finally, conclusions and discussion are given in the last section.

II. Description of the Wire-Frame Method

Consider a blending surface that joins two primary surfaces in three dimensional space. To smoothly join the two primary surfaces, the intersections of the primary surfaces and the blending surface should be continuous and their derivatives should also be continuous. That is, the blending surface must meet the containment and tangency requirements. In other words, if we consider the primary surfaces and the blending surface as one function, it is a C^1 continuous function (Choi, 1991; Hoffmann and Hopcroft, 1985).

Suppose that G and H are the two primary surfaces to be blended at the transversals T and T', respectively. The blending surface generated using the wire-frame method is a set of bicubic patches. Our method first constructs a set of wire frames. We distinguish two types of wire frames. Those wire frames from T to T' are called *latitudinal wire frames* while those "parallel" to T and T' are called *longitudinal wire frames*.

We first show how to model latitudinal wire frames. Longitudinal wire frames can be modeled in a similar way. Select pairs of matching points on T and T'. Let the selected points on T be A, B, C etc, and their corresponding points on T' be A', B', C' etc.

Each pair of matching points is connected by a smooth curve. These curves are the latitudinal wire frames. Take the pair of points A and A' as an example. Denote the curves from A to A' by

$$\{(x(s), y(s), z(s))|0\le s\le 1\}. \quad \textbf{(1)}$$

Let (x_0, y_0, z_0) be the coordinates of the point A, and let (x_1, y_1, z_1) be the coordinates of the point A'. Let $t_x(0)$, $t_y(0)$, $t_z(0)$, and $t_x(1)$, $t_y(1)$, $t_z(1)$ be the derivatives at point A and A' along the x-, y-, and z-axis, respectively. The containment and tangent requirements can be written as

$$x(0)=x_0,\ x(1)=x_1,$$

$$y(0)=y_0,\ y(1)=y_1,$$

$$z(0)=z_0,\ z(1)=z_1, \quad \textbf{(2)}$$

and

$$\begin{pmatrix} dx/ds \\ dy/ds \\ dz/ds \end{pmatrix} = \alpha_s \begin{pmatrix} t_x(s) \\ t_y(s) \\ t_z(s) \end{pmatrix} \text{ at } s=0,1, \quad \textbf{(3)}$$

where α_0 and α_1 are nonzero constants.

Next, we show how to find a set of functions, $x(s)$, $y(s)$, and $z(s)$, to satisfy Eqs. (2) and (3), that is, to satisfy the continuity and the derivative continuity requirements. One possible way is to solicit a fourth-order ordinary differential equation.

Consider an elastic beam clamped at both ends. The deflection $u(s)$ satisfies the following equation:

$$\frac{d^2}{ds^2}[p(s)\frac{d^2}{ds^2}u(s)] = f(s), \ 0 \le s \le 1, \quad \textbf{(4)}$$

where $p(s)$ is the bending stiffness and $f(s)$ is the external load per unit length. In order to apply the finite element method, Eq. (4) is rewritten as the following weak formulation:

$$\min \{\frac{1}{2}\int_0^1 p(s)[\frac{d^2}{ds^2}v(s)]^2 ds - \int_0^1 f(s)v(s)ds\}, \quad \textbf{(5)}$$

where $v(s) \in C^1[0,1]$, which satisfies

$$v(0)=v_0, \qquad v(1)=v_1,$$

$$\frac{d}{ds}v(0) = v_0', \quad \frac{d}{ds}v(1) = v_1'. \quad \textbf{(6)}$$

III. A Numerical Solution for the Wire-Frame Method

In this section, we present a numerical solution for the wire-frame method. We first show how to compute the latitudinal wire frames, and then we show how to compute the longitudinal wire frames. After both wire frames are computed, a set of bicubic patches that represent the blending surface can be computed.

1. Construction of Latitudinal Wire Frames

Note that $x(s)$, $y(s)$, and $z(s)$ must satisfy the boundary conditions defined by Eq. (3). We first show how the tangency requirement can be satisfied by the parametric equations, that is, how the values of $\frac{dx}{ds}$, $\frac{dy}{ds}$, and $\frac{dz}{ds}$ can be determined. This technique was also used in Bajaj and Ihm's method (Bajaj and Ihm, 1992):

(1) If $t_x \neq 0$, choose $t_x\frac{dy}{ds}=t_y\frac{dx}{ds}$, $t_x\frac{dz}{ds}=t_z\frac{dx}{ds}$.

(2) If $t_y \neq 0$, choose $t_y\frac{dx}{ds}=t_x\frac{dy}{ds}$, $t_y\frac{dz}{ds}=t_z\frac{dy}{ds}$.

(3) If $t_z \neq 0$, choose $t_z\frac{dx}{ds}=t_x\frac{dz}{ds}$, $t_z\frac{dy}{ds}=t_y\frac{dz}{ds}$.

For example, assume that $t_x \neq 0$ at $s=0$, and that $t_y \neq 0$ at $s=1$. We may choose an arbitrary $dx(0)/ds$ and then obtain $dy(0)/ds$ and $dz(0)/ds$. Similarly, we may choose $dy(1)/ds$ and compute the values of $dx(1)/ds$ and $dz(1)/ds$. Now we have a vector of the form

$$\overrightarrow{W} = (\frac{dx}{ds}\Big|_{s=0}, \frac{dy}{ds}\Big|_{s=1})^T \quad \textbf{(7)}$$

to be determined. Since the surface has no singularity,

$$\begin{pmatrix} dx/ds \\ dy/ds \\ dz/ds \end{pmatrix} \neq \overrightarrow{0}. \quad \textbf{(8)}$$

The two vector components in Eq. (7) can never be zero. When $t_x=0$ at $s=0$, or when $t_y=0$ at $s=1$, we may choose another component which is not equal to zero and then find the values of the other derivatives.

There are two parameters that can be chosen arbitrarily. To obtain a general solution to the differential equation, we may choose three linear independent trial vectors, such as

$$\overrightarrow{W}_I = (1,1), \ \overrightarrow{W}_{II} = (1,-1), \ \overrightarrow{W}_{III} = (-1,1). \quad \textbf{(9)}$$

This allows us to solve the three functions $x(s)$, $y(s)$, and $z(s)$ of Eq. (1) separately. For example, we can solve $x(s)$ by minimizing

$$\int_0^1 p(s)\frac{d^2}{ds^2}x(s)\frac{d^2}{ds^2}v(s)ds = \int_0^1 f(s)v(s)ds, \quad \textbf{(10)}$$

where $x \in H_*^2(s)$, $v \in H_0^2(s)$. Note that $H_*^2(s)$ is the set of functions in $H^2(s)$ satisfying

$$x(0)=x_0, \ x(1)=x_1, \ x'(0)=t_x(0), \ x'(1)=t_x(1), \quad \textbf{(11)}$$

and that $H_0^2(s) \subset H^2(s)$ is the set of functions satisfying the homogeneous conditions:

$$x(0)=x(1)=x'(0)=x'(1)=0. \quad \textbf{(12)}$$

Here $H^2(s)$ is the *Solobev space*, and $v \in C^1(s)$. That is, the derivatives dv/ds are continuous. We next choose the Hermite element:

$$\varphi_0^0(s) = 2\overline{s}^3 - 3\overline{s}^2 + 1,$$

$$\varphi_0^1(s) = \overline{s}^3 - 2\overline{s}^2 + \overline{s},$$

$$\varphi_1^0(s) = -2\overline{s}^3 + 3\overline{s}^2,$$

$$\varphi_1^1(s) = \overline{s}^3 - \overline{s}^2 . \quad \textbf{(13)}$$

We divide the interval [0,1) quasi-uniformly into $N-1$ subintervals and denote them by $s_1, s_2, \ldots, s_N$. Then the transformation is

$$s = s_i + \overline{s}\, h_i \quad \text{or} \quad \overline{s} = \frac{s - s_i}{h_i}$$

and

$$\frac{d\varphi}{d\overline{s}} = \frac{d\varphi}{ds}\frac{ds}{d\overline{s}} = \frac{d\varphi}{ds} h_i$$

where $h_i = s_{i+1} - s_i$. We choose the function on $[s_i, s_{i+1})$ as defined by Carey and Oden (1983):

$$x_h^i(s) = x_i \varphi_0^0(\overline{s}) + x_{i+1}\varphi_1^0(\overline{s}) + [x_i' \varphi_0^1(\overline{s}) + x_{i+1}' \varphi_1^1(\overline{s})] h_i$$

$$= x_i \varphi_0^0\left(\frac{s - s_i}{h_i}\right) + x_{i+1}\varphi_1^0\left(\frac{s - s_i}{h_i}\right)$$

$$+ h_i\left[x_i' \varphi_0^1\left(\frac{s - s_i}{h_i}\right) + x_{i+1}' \varphi_1^1\left(\frac{s - s_i}{h_i}\right)\right]. \quad \textbf{(14)}$$

The piecewise functions are

$$x_h(s) = \sum_{i=1}^{N} x_h^i(s) = \sum_{i=0}^{N-1}\left[\sum_{k=0}^{1} x_{i+k}\varphi_k^0\left(\frac{s - s_i}{h_i}\right)\right.$$

$$\left. + h_i \sum_{k=0}^{1} x_{i+k}' \varphi_k^1\left(\frac{s - s_i}{h_i}\right)\right]. \quad \textbf{(15)}$$

The finite element method can then be applied to compute the values of the unknowns x_i and x_i', for $i=1, 2, \ldots, N-1$, which satisfy

$$\int_0^1 p(s)\frac{d^2}{ds^2}x_n(s)\frac{d^2}{ds^2}v_n(s)ds = \int_0^1 f(s)v_n(s)ds . \quad \textbf{(16)}$$

That is, we obtain a system of $2N-2$ linear equations:

$$A\overline{X} = \overline{F}, \quad \textbf{(17)}$$

where A is a $(2N-2)\times(2N-2)$ symmetric and positive definite matrix. The unknowns x_i and x_i', $i=1, 2, \ldots, N-1$ can be obtained easily by solving Eq. (17) (see Guan and Li (1996) for details).

After obtaining (x_i, x_i'), (y_i, y_i'), and (z_i, z_i'), for two trial vectors in Eq. (9), we can construct a general solution:

$$X_n(s) = aX_n^I(s) + bX_n^{II}(s) + cX_n^{III}(s)$$

$$Y_n(s) = aY_n^I(s) + bY_n^{II}(s) + cY_n^{III}(s)$$

$$Z_n(s) = aZ_n^I(s) + bZ_n^{II}(s) + cZ_n^{III}(s) ,$$

where $X_n^I(s)$, X_n^{II}, and $X_n^{III}(s)$ are the solutions to Eq. (16) under the conditions in Eq. (9), respectively. Since $a+b+c=1$, we obtain

$$X_n(s) = aX_n^I(s) + bX_n^{II}(s) + (1-a-b)X_n^{III}(s)$$

$$Y_n(s) = aY_n^I(s) + bY_n^{II}(s) + (1-a-b)Y_n^{III}(s)$$

$$Z_n(s) = aZ_n^I(s) + bZ_n^{II}(s) + (1-a-b)Z_n^{III}(s) .$$

Therefore, we only have two degrees of freedom, the parameters a and b, which need to be determined. In another paper, we present a technique for obtaining an optimal curve based on minimization of the global energy (Guan and Li, 1996).

In the above algorithm, we need to apply the finite element method to Eq. (16) 9 times. For n curves, we need to solve Eq. (17) $9n$ times. Fortunately, since the matrix A can be chosen equally, we may use the Cholesky decomposition to decompose the matrix A. Let

$$A = L^T T, \quad \textbf{(18)}$$

where L is a unit lower triangular matrix and T is an upper triangular matrix. The matrices L and T can be stored for repeated use. We can solve different equations by using different F_i. Since $A\overline{X}_i = L^T(T\overline{X}_i) = \overline{F}_i$, we let $T\overline{X}_i = \overline{U}_i$, $L^T\overline{U}_i = \overline{F}_i$. Therefore,

$$L^T\overline{U}_i = \overline{F}_i \quad \textbf{(19)}$$

$$T\overline{X}_i = \overline{U}_i . \quad \textbf{(20)}$$

We only need to decompose Eq. (18) once and use the same decomposition to obtain all the solutions. This greatly reduces the computational cost.

The above algorithm coincides with the geometric intuition of blending an elastic beam clamped at its boundary. It is interesting to note that the bending stiffness $p(s)$ and the load $f(s)$ can be used to control the shape of the blending surfaces.

2. Construction of Longitudinal Wire Frames

We use polar coordinates (r,θ) in the construction of longitudinal wire frames. Let the centers of the coordinates of T and T' be O and O', respectively.

Suppose that the sequences of points A, B, C, ... and A', B', C', ... are both located on T and T' in a counter-clockwise direction so that the global blending surface can be coherent. Otherwise, we may obtain ill-twisted blending surfaces. Assign a coordinate θ_i to each latitudinal wire frame obtained in the previous section.

We know the coordinates of the points $x_{i,j}$, and their derivatives $\frac{d}{ds}x_{i,j}$, where $x_{i,j}=x(s_i,\theta_j)$. We will now show how to construct smooth curves $x_i(\theta)$, $0\le\theta\le 2\pi$, for each i=1, 2, ..., N. Consider the piecewise cubic functions of Eq. (13):

$$\overline{\theta}=\frac{\theta-\theta_j}{\Delta\theta_j},$$

where

$$\Delta\theta_j=\theta_{j+1}-\theta_j.$$

$$\varphi_0^0(\overline{\theta})=2\overline{\theta}^3-3\overline{\theta}^2+1,$$

$$\varphi_0^1(\overline{\theta})=\overline{\theta}^3-2\overline{\theta}^2+\overline{\theta},\qquad \overline{\theta}\in[0,1)$$

$$\varphi_1^0(\overline{\theta})=-2\overline{\theta}^3+3\overline{\theta}^2$$

$$\varphi_1^1(\overline{\theta})=\overline{\theta}^3-\overline{\theta}^2. \qquad \textbf{(21)}$$

Let M be the number of partitions along θ; then $\theta_0=0$, and $\theta_M\le 2\pi$. The jth smooth curves can be written as

$$x_{i,h}(\theta)=x_h^j(\theta)=\sum_{j=0}^{M}x_h^{i,j}(\theta)=\sum_{j=1}^{M}\Big[\sum_{k=0}^{1}x_{i,j+k}\varphi_k^0\Big(\frac{\theta-\theta_j}{\Delta\theta_j}\Big)+\Delta\theta_j\sum_{k=0}^{1}\frac{\partial}{\partial\theta}x_{i,j+k}\varphi_k^1\Big(\frac{\theta-\theta_j}{\Delta\theta_j}\Big)\Big]. \qquad \textbf{(22)}$$

The values of $x_{i,j}$ are known, but those of $\partial x_{i,j}/\partial\theta$ are unknown. However, we may compute these values from Eq. (5). Hence, Eq. (10) is modified as

$$\int_0^{2\pi}p(\theta)\frac{\partial^2}{\partial\theta^2}x(\theta)\frac{\partial^2}{\partial\theta^2}v(\theta)d\theta=\int_0^{2\pi}f_i^*(\theta)v(\theta)d\theta. \qquad \textbf{(23)}$$

We substitute Eq. (22) for $x_i(\theta)$

$$\int_0^{2\pi}p(\theta)\frac{\partial^2}{\partial\theta^2}x_{i,h}(\theta)\frac{\partial^2}{\partial\theta^2}v_{i,h}^*d\theta=\int_0^{2\pi}f_i^*(\theta)v_{i,h}^*(\theta)d\theta, \qquad \textbf{(24)}$$

where the functions $v_{i,h}^*$ satisfy Eq. (22) with the homogeneous boundary conditions $x_{i,j}=0$, j=0, 1, ..., M. The finite element method can be applied to solve for $\frac{\partial x_{i,j}}{\partial\theta}$. The values of $\frac{\partial^2 x_{i,j}}{\partial\theta\partial s}$ can be obtained in a similar way.

Consider the following different boundary conditions:

(1) The curves $x_i(\theta)$ are not closed.
Since $\theta_M=\overline{\theta}\le 2\pi$, two cases may occur.
(i) No normal derivatives are given.
Then the values $\frac{\partial}{\partial\theta}x_{i,0}$ and $\frac{\partial}{\partial\theta}x_{i,M}$ can be obtained by solving Eq. (24).
(ii) The derivatives $\frac{\partial}{\partial\theta}x_{i,0}=h_{i,0}$ and $\frac{\partial}{\partial\theta}x_{i,M}=h_{i,M}$ are given.
The other $M-1$ derivatives $\frac{\partial}{\partial\theta}x_{i,j}$, j=1, 2, ..., $M-1$ can be obtained by solving Eq. (24).
(2) The curves $x_i(\theta)$ are closed.
Then $x_{i,0}=x_{i,M}$, and $\frac{\partial}{\partial\theta}x_{i,0}=\frac{\partial}{\partial\theta}x_{i,M}$. The M derivatives $\frac{\partial}{\partial\theta}x_{i,j}$, j=1, 2,...., M can also be obtained by solving Eq. (24).

Finally, we can use the known $\frac{\partial}{\partial s}x_{i,j}$ and follow the above procedure for solving an ordinary differential equation, to obtain $\frac{\partial^2}{\partial\theta ds}x_{i,j}$.

Another method for computing the values of $\frac{\partial x_{i,j}}{\partial\theta}$ and $\frac{\partial^2 x_{i,j}}{\partial\theta\partial s}$ is to compute $w(s)=\frac{\partial x}{\partial\theta}$, where s is measured along the latitudinal wire frames. The equation we want to solve is

$$\frac{d^2}{ds^2}\Big[p(s)\frac{d^2}{dr^2}w(s)\Big]=f(s).$$

The boundary conditions are $\frac{\partial x_{i,j}}{\partial\theta}=x'_{i,j}$ and $\frac{\partial^2 x_{i,j}}{\partial\theta\partial s}=x''_{i,j}$, j=0, 1, ..., M. The values of $x'_{i,0}$ and $x'_{i,M}$ are given by the boundaries of the blending surface. The values of $x''_{i,0}$ and $x''_{i,M}$ can be chosen to be 0 for the general case. The method described in Section III.1 can then be used to obtain $\frac{\partial x_{i,j}}{\partial\theta}$ and $\frac{\partial^2 x_{i,j}}{\partial\theta\partial s}$ simultaneously. However, the band-width of the matrix generated using this approach is at least twice as large as the one generated using the first method. Therefore, this approach may need more computational time.

3. Compute Bicubic Patches for the Blending Surfaces

So far, we have found the values $x_{i,j}$, $\frac{\partial}{\partial s}x_{i,j}$, $\frac{\partial}{\partial\theta}x_{i,j}$, and $\frac{\partial^2}{\partial\theta\partial s}x_{i,j}$, where $x_{i,j}=x(s_i,\theta_j)$, i=0, 1, ..., N, and j=0, 1, ..., M. Consider the "rectangle" $\Omega_{i,j}[s_i\le s<s_{i+1}$, $\theta_j\le\theta<\theta_{j+1}]$. Applying the tensor product of Carey and Oden (1983), we obtain the bicubic Hermite interpolations on the unit square $[0,1]\times[0,1]$:

$$u(\overline{s},\overline{\theta})=\sum_{k,l=0}^{1}x_{kl}\varphi_k(\overline{s})\varphi_l(\overline{\theta})+\sum_{k,l=0}^{1}\Big(\frac{\partial}{\partial s}x_{kl}\Big)\varphi_k(\overline{s})\varphi_l(\overline{\theta})$$

$$+\sum_{k,l=0}^{1}\left(\frac{\partial}{\partial\theta}x_{k,l}\right)\varphi_k(\bar{s})\varphi_l(\bar{\theta})$$

$$+\sum_{k,l=0}^{1}\left(\frac{\partial^2}{\partial\theta\partial s}x_{k,l}\right)\varphi_k(\bar{s})\varphi_l(\bar{\theta}),$$

where

$$\varphi_0^0(\bar{s})=2\bar{s}^3-3\bar{s}^2+1,$$

$$\varphi_0^1(\bar{s})=\bar{s}^3-2\bar{s}^2+\bar{s},$$

$$\varphi_1^0(\bar{s})=-2\bar{s}^3+3\bar{s}^2,$$

$$\varphi_1^1(\bar{s})=\bar{s}^3-\bar{s}^2.$$

The entire surface is composed of

$$\begin{aligned}x_h(s,\theta)=\sum_{i=0}^{N-1}\sum_{j=0}^{M-1}\Big[&\sum_{k,l=0}^{1}x_{i+k,j+l}\varphi_{i,k}^0(s)\varphi_{j,l}^0(\theta)\\&+h_i\sum_{k,l=0}^{1}\left(\frac{\partial}{\partial s}x_{i+k,j+l}\right)\varphi_{i,k}^1(s)\varphi_{j,l}^0(\theta)\\&+\Delta\theta_j\sum_{k,l=0}^{1}\left(\frac{\partial}{\partial\theta}x_{i+k,j+l}\right)\varphi_{i,k}^0(s)\varphi_{j,l}^1(\theta)\\&+h_i\Delta\theta_j\sum_{k,l=0}^{1}\left(\frac{\partial^2}{\partial s\partial\theta}x_{i+k,j+l}\right)\varphi_{i,k}^1(s)\varphi_{j,l}^1(\theta)\Big],\end{aligned}\quad\textbf{(25)}$$

where

$$\varphi_{i,k}^0(s)=\varphi_k^0\left(\frac{s-s_i}{h_i}\right),\ \varphi_{j,l}^0(\theta)=\varphi_l^0\left(\frac{\theta-\theta_j}{\Delta\theta_j}\right),$$

$$\varphi_{i,k}^1(s)=\varphi_{k+1}^1\left(\frac{s-s_i}{h_i}\right),\ \varphi_{j,l}^1(\theta)=\varphi_l^1\left(\frac{\theta-\theta_j}{\Delta\theta_j}\right).$$

It can be shown that the solutions in Section III are the same as that for Eq. (25) along the wire-frame $s=s_i$ and $\theta=\theta_j$, and that $x_n(s,\theta)\in C^1$, satisfying the boundary conditions.

The tensor-product form of Eq. (25) can be expressed in matrix-vector form (Li, 1994):

$$x(s,\theta)=\bar{S}\,CPC^T\bar{Q},$$

where

$$\bar{S}=(s^3,s^2,s,1)^T,\ \bar{\Theta}=(\theta^3,\theta^2,\theta,1)^T,\ s\in[0,1),\ \theta\in[0,1)$$

and

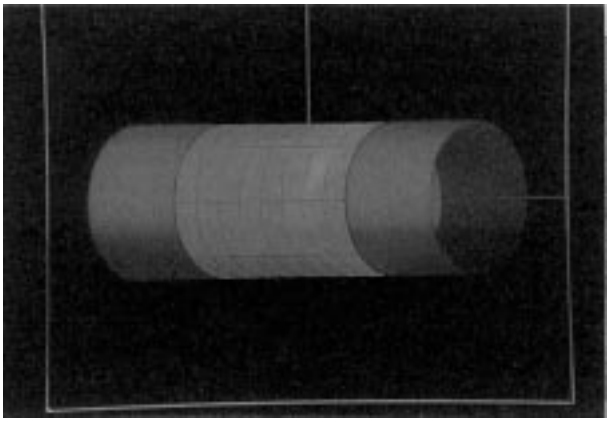

Fig. 1. Choose the corresponding pairs of points in a suitable way.

$$P=\begin{bmatrix}x_{00} & x_{01} & \partial x_{00}/\partial\theta & \partial x_{01}/\partial\theta\\ x_{10} & x_{11} & \partial x_{10}/\partial\theta & \partial x_{11}/\partial\theta\\ \partial x_{00}/\partial r & \partial x_{01}/\partial r & \partial x_{00}^2/\partial r\partial\theta & \partial x_{01}^2/\partial r\partial\theta\\ \partial x_{10}/\partial r & \partial x_{11}/\partial r & \partial x_{10}^2/\partial r\partial\theta & \partial x_{11}^2/\partial r\partial\theta\end{bmatrix}$$

and

$$C=\begin{bmatrix}2&-2&1&1\\-3&3&-2&-1\\0&0&1&0\\1&0&0&0\end{bmatrix}.$$

IV. Examples

In this section, we give some examples produced using the wire-frame method with the functions $p(s)=1$ and $f(s)=0$ and $\alpha=1$. Note that for such simple cases, the particular solutions of the ordinary differential equations can be obtained explicitly (Guan and Li, 1996). Here we use these cases to demonstrate the versatility of our algorithms. First, we compare results obtained using different choices of connecting points for the latitudinal wire frames. Assume that the two primary surfaces are of the same radius and have the same axis. The results are shown in Fig. 1. Their parametric representations are as follows:

G: $(5\cos\theta,\ 5\sin\theta,\ z)$ $\hat{G}$: $z=5$

H: $(5\cos\theta,\ 5\sin\theta,\ z)$ $\hat{H}$: $z=-5$.

With the same primary surfaces and clip surfaces, we choose the corresponding pairs of points on the primary

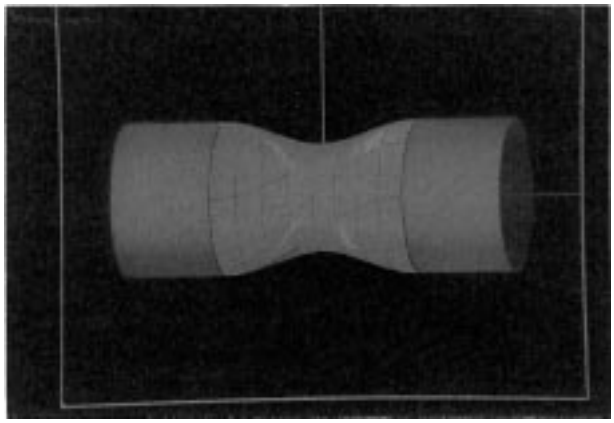

Fig. 2. Choose the corresponding pairs of points which rotate $\pi/2$.

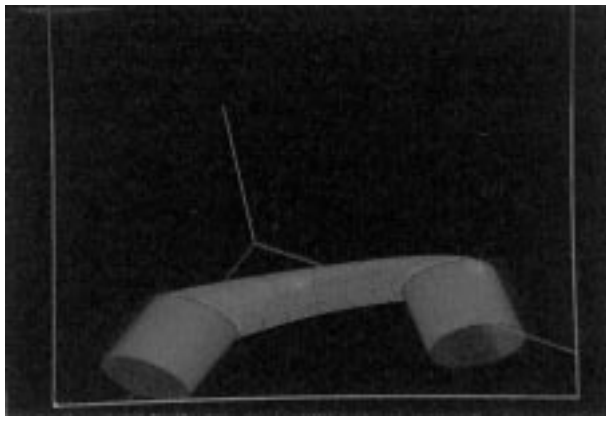

Fig. 4. Blending with a small tangent vector.

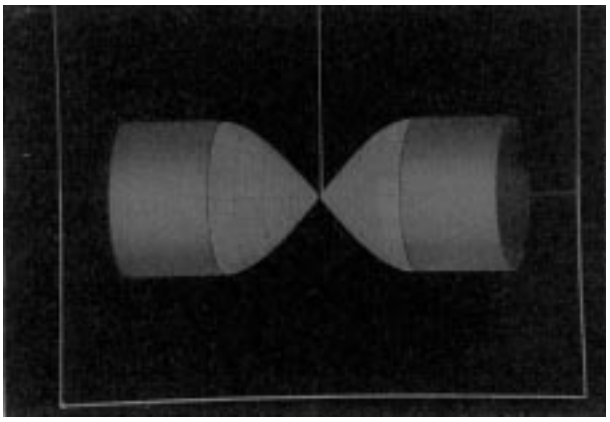

Fig. 3. Choose the corresponding pairs of points which rotate π.

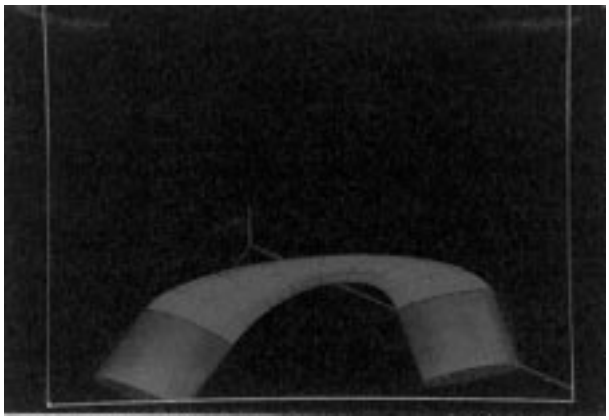

Fig. 5. Blending with a large tangent vector.

surfaces in different ways. The primary surfaces for Fig. 2 are

G: $(5\cos\theta,\ 5\sin\theta, z)$ $\quad\hat{G}$: $z=5$

H: $(5\cos(\theta+\pi/2),\ 5\sin(\theta+\pi/2), z)$ $\quad\hat{H}$: $z=-5$,

and those for Fig. 3 are

G: $(5\cos\theta,\ 5\sin\theta, z)$ $\quad\hat{G}$: $z=5$

H: $(5\cos(\theta+\pi),\ 5\sin(\theta+\pi), z)$ $\quad\hat{H}$: $z=-5$.

Next, we compare the results obtained using different magnitudes of tangent vectors. We generate the blending surfaces for two cylinders with different axes as shown in the examples. See Figs. 4 and 5. These figures have the same primary surfaces and clip surfaces, but they differ in the magnitudes of the tangent vectors. The parametric representations of Fig. 4 are as follows:

G: $(2\cos\theta,\ 2\sin\theta,\ z)$ $\quad\hat{G}$: $z=5$

$$H: \left(\frac{7+2\cos(\theta+\pi)+z}{\sqrt{2}}, -2\sin(\theta+\pi),\right.$$

$$\left.\frac{-7-2\cos(\theta+\pi)+z}{\sqrt{2}}\right) \qquad \hat{H}: x+z=-5.$$

Third, we compare the results obtained using different numbers of longitudinal wire frames. We choose the number M to be 4 and 8, and the results are shown in Figs. 6 and 7. The parametric representations of these figures are

G: $(2\cos\theta,\ 2\sin\theta, z)$ $\quad\hat{G}$: $z=5$

H: $(x,\ 6\sin\theta,\ 6\cos\theta)$ $\quad\hat{H}$: $x^2+y^2=16$.

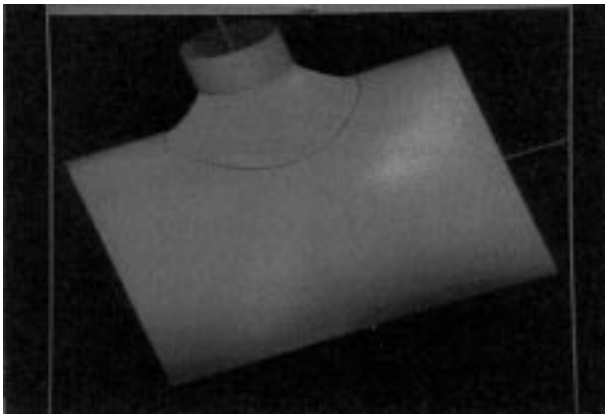

Fig. 6. Blending with 4 longitudinal wire frames.

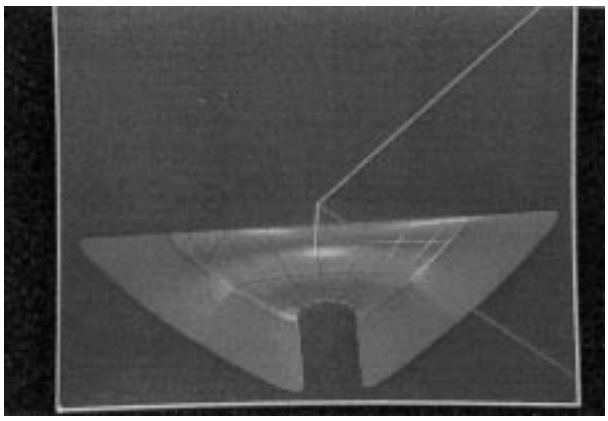

Fig. 8. Blending surface for two different cones.

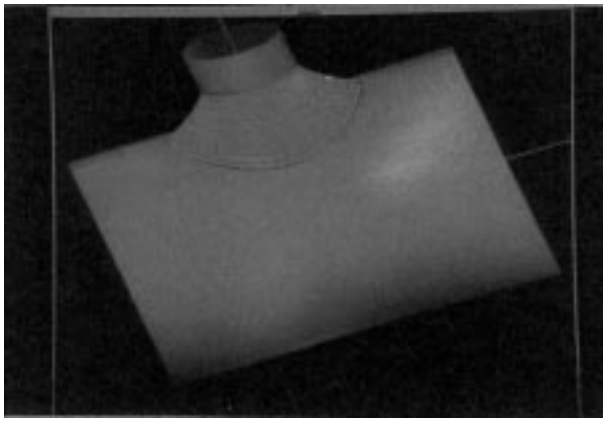

Fig. 7. Blending with 8 longitudinal wire frames.

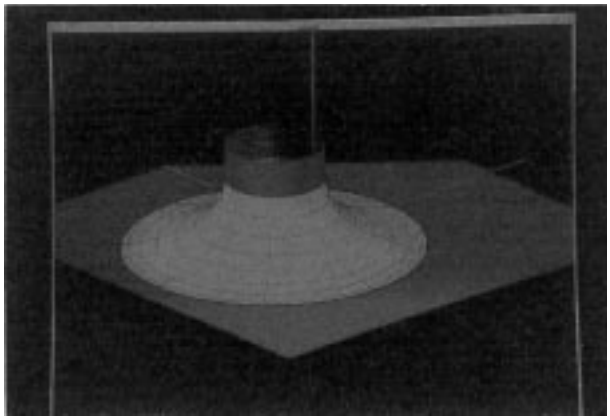

Fig. 9. Blending surface for a cylinder and a plane.

Finally, we show several combination of primary surfaces. Figure 8 gives an example in which the primary surfaces are cones.

Figure 9 gives an example in which one primary surface is a plane and the other surface is a cylinder.

Figure 10 gives an example in which two primary surfaces are cylinders with different radii.

The last example, Fig. 11, shows that the wire-frame method can also be used in the case where the primary surfaces are not closed.

V. Conclusions and Discussion

We have presented a wire-frame method for the design of blending surfaces. We first summarize the wire-frame method as follows.

Each latitudinal wire-frame is modeled by a loaded thin elastic beam clamped at both ends. The deflection of the beam can be computed by solving a fourth order ordinary differential equation. Therefore, for i=1, 2, ..., N, the points and their derivatives along the i-th latitudinal wire-frame,

$$x_{ij},\ \frac{d}{ds}x_{ij},\ 0\le j\le M,$$

can be calculated. Based on these values, the longitudinal wire-frame is modeled using polar coordinates. By solving a similar fourth order ordinary differential equation, we can obtain the values of

$$\frac{\partial}{\partial\theta}x_{ij},\ \frac{\partial^2}{\partial\theta\partial s}x_{ij},\ 0\le i\le N\ 0\le j\le M.$$

For each rectangle defined by the points on the wire-frames, a bicubic patch for the blending surface can then be computed using the tensor-product rule.

The wire-frame method provides great flexibility in the design of blending surfaces. Since the ordinary differential equation is based on elastic bending beams, curves generated using our method have minimum

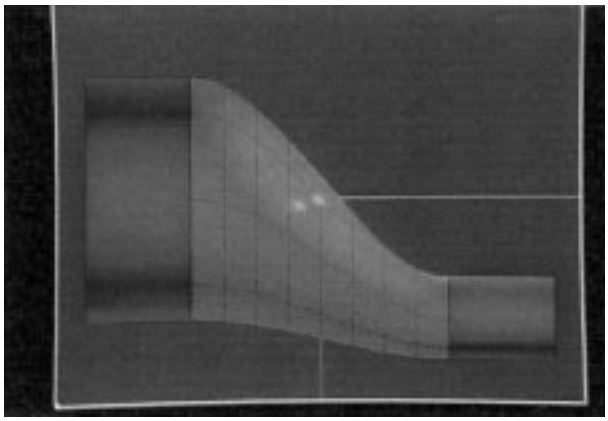

Fig. 10. Blending surface for two cylinders with different radii.

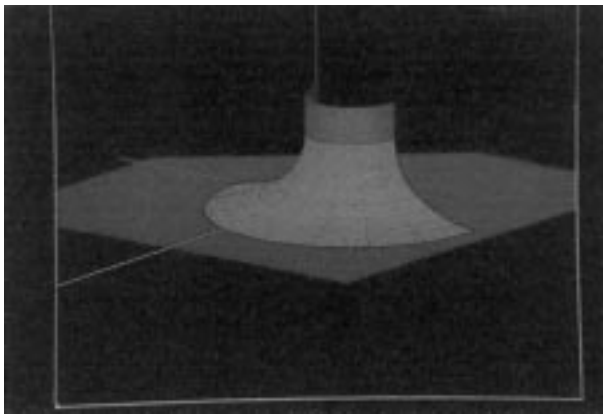

Fig. 11. Blending surface for open primary surfaces.

curvatures. That is, the second-order derivatives are as small as possible (Fisher, 1994; Su and Lin, 1989). This guarantees a good geometric property of the blending surfaces. The two primary surfaces to be blended can be of any algebraic degree and in any position. The shape of the blending surface can be controlled by adjusting the stiffness of the beam and the external load added to the beam. This concept coincides with the experience of design engineers and helps the designer control the shape of the blending surfaces. The wire-frame method also is suitable for finite element analysis. Therefore, stress strain analysis, fluid flow analysis and other types of analysis can easily be incorporated.

To apply the wire-frame method in the design of blending surfaces, we need the finite element method and interpolation. The theory of the finite element method can be found in Becker *et al*. (1981) and Carey and Oden (1983). Implementation of the finite element method in blending surface design is simple, and computation is quite fast. After the wire-frame of a blending surface is determined, a set of piecewise bicubic patches that represent the blending surface can be obtained from the interpolating polynomials using the tensor-product rule. The computation can be found, for example, in Choi's book on surface modeling for CAD/CAM (Choi, 1991), in Gregory's book on the mathematics of surfaces (Gregory, 1986), in Su and Liu's book on curves and surface modeling (Su and Lin, 1989) or in Koenderink's book on solid shapes (Koenderink, 1990). All the tools needed in the wire-frame method have been well developed.

In the case where the primary surfaces are not in cubic parametric form, there will be some gaps between the two primary surfaces and the blending surfaces. Choosing more latitudinal and longitudinal frames can reduce the gaps but will also increase the complexity of the blending surfaces. For detailed error analysis and the rate of convergence, see Guan and Li (1996) and Li (1996). On the other hand, if the primary surfaces are low degree polynomials, then finite element methods need not be applied. Analytical solutions can be obtained for these surfaces.

Care must be taken in choosing pairs of matching points in the construction of latitudinal wire frames. This difficulty arises in most algorithms for parametric representation of surfaces. In some cases, there is a natural way to find the matching pairs. For example, when the blending surface is used to join two cylinders, a set of matching points can be obtained by rotating a plane along the axis of the cylinder with smaller diameter. In general, there are four intersection points for each position of the rotating plane and the transition curves T and T'. It is easy to pair up these four points. When the transition curves T and T' are irregular, we can first find points that are the centers of the two curves. (Let P be a point and T be a curve. Define that $r(P)=\max\{d(P,X)|X$ is a point on the curve $T\}$. A center of a curve is defined as the point P with the minimum $r(P)$.) However, rotating a plane along the line that passes through the two centers may generate more than four intersection points, and the matching pairs may be difficult to determine. Care must also be taken not to generate a set of twisted latitudinal wire-frames (see, for example, Figs. 2 and 3). Although twisted latitudinal wire-frames may be useful in some cases, they should be avoided in general.

The wire-frame method is suitable for joining two surfaces. Some modifications are needed to blend corners, where more than two surfaces join together. We may use a similar procedure for latitudinal and longitudinal wire frames and then apply triangular patches in the vertex region as stated by Choi (1991). In this case, the choices of boundary points and their

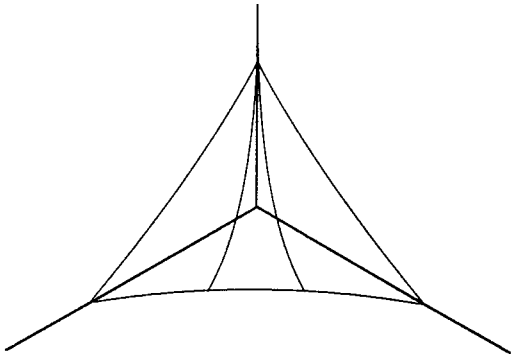

Fig. 12. Blending of corners.

matchings are crucial. A method for choosing these points is illustrated in Fig. 12.

Acknowledgment

This research was supported in part by the National Science Council of the Republic of China under grant NSC 84-2121-M-110-003-MS and grant NSC 84-2121-M-110-006-MS.

References

Bajaj, C. L. and I. Ihm (1992) Algebraic surface design with hermite interpolation. *ACM Transactions on Graphics*, **11**(1), 61-91.

Becker, E. B., G. F. Carey, and J. T. Oden (1981) *Finite Element, an Introduction*, Vol. I. Prentice-Hall Inc., New York, NY, U.S.A.

Bloor, M. I. G. and M. J. Wilson (1989) Generating blend surfaces using partial differential equations. *Computer Aided Design*, **21**(3), 165-171.

Bloor, M. I. G. and M. J. Wilson (1990a) Representing PDE surfaces in terms of B-splines. *Computer Aided Design*, **22**(6), 324-330.

Bloor, M. I. G. and M. J. Wilson (1990b) Using partial differential equations to generate free-from surfaces. *Computer Aided Design*, **22**(4), 202-212.

Carey, G. F. and J. T. Oden (1983) *Finite Element, a Second Course*, Vol. II. Prentice-Hall Inc., New York, NY, U.S.A.

Celniker, G. and D. Gossard (1991) Deformable curve and surface finite-elements for free-form shape design. *Computer Graphics*, **25**(4), 257-265.

Choi, B. K. (1991) *Surface Modelling for CAD/CAM*. Elsever, Amsterdam, Netherlands.

Filip, D. J. (1989) Blending parametric surfaces. *ACM Transactions on Graphics*, **8**(3), 164-173.

Fisher, R. B., Ed. (1994) *Design and Application of Curves and Surfaces*. Oxford University Press, Oxford, U.K.

Gregory, J. A., Ed. (1986) *The Mathematics of Surfaces*. Clarendon Press, Oxford, U.K.

Guan, D. J. and Z. C. Li (1996) *Solution of Differential Equations for Blending Curves*. Technical report, Department of Applied Mathematics, National Sun Yat-Sen University, Kaohsiung, Taiwan, R.O.C.

Hoffmann, C. and J. Hopcroft (1985) Automatic surface generation in computer aided design. *The Visual Computer*, **1**, 92-100.

Hoffmann, C. and J. Hopcroft (1986) Quadratic blending surfaces. *Computer Aided Design*, **18**(6), 301-306.

Hoffmann, C. and J. Hopcroft (1987) The potential method for blending surfaces and corners. In: *Geometric Modeling*, pp. 347-366. G. Farin Ed. SIAM, Philadelphia, PA, U.S.A.

Hoffmann, C. and J. Hopcroft (1988) The geometry of projective blending surfaces. *Artificial Intelligence*, **37**, 357-376.

Holmström, L. (1987) Piecewise quadric blending of implicitly defined surfaces. *Computer Aided Geometric Design*, **4**, 171-189.

Kallay, M. and B. Ravani (1990) Optimal twist vectors as a tool for interpolating a network of curves with minimum energy surface. *Computer Aided Geometric Design*, **7**, 465-473.

Koenderink, J. J. (1990) *Solid Shape*. The MIT Press, Cambridge, MA, U.S.A.

Kosters, M. (1989) Quadratic blending surfaces for corners. *The Visual Computer*, **5**, 134-146.

Li, Z. C. (1994) Advanced splitting integrating methods with high converge rates for restoring images and patterns. *Journal of Scientific Computing*, **9**, 149-172.

Li, Z. C. (1996) Boundary Penalty Finite Element Method for Blending Surfaces. Technical Report, Department of Applied Mathematics, National Sun Yat-Sen University, Kaohsiung, Taiwan, R.O.C.

Lounsbery, M., S. Mann, and T. DeRose (1992) Parametric surface interpolation. *IEEE Computer Graphics and Applications*, **1**, 45-52.

Moreton, H. P. and C. H. Séquin (1992) Functional optimization for fair surface design. *Computer Graphics*, **26**(2), 167-176.

Nielson, G. M. (1980) Minimum norm interpolation in triangles. *SIAM Journal on Numerical Analysis*, **17**(1), 44-62.

Nielson, G. M. (1983) A method for interpolating scatered data based upon a minimum norm network. *Mathematics of Computation*, **40**(161), 257-265.

Ohkura, K. and Y. Kakazu (1992) Generalization of the potential method for blending three surfaces. *Computer Aided Design*, **24**(11), 599-612.

Su, B. Q. and D. Y. Lin (1989) *Computational Geometry, Curves and Surfaces Modeling*. Academic Press Inc., San Diego, CA, U.S.A.

Vida, J., R. R. Martin, and T. Varady (1994) A survey of blending methods that use parametric surfaces. *Computer Aided Design*, **26**(5), 341-364.

Warren, J. (1987) Blending quadric surfaces with quadric and cubic surfaces. *Proceedings of the ACM Symposium on Computer Geometry Design*, pp. 342-347. ACM, New York, NY, U.S.A.

Warren, J. (1989) Blending algebraic surfaces. *ACM Transactions on Graphics*, **8**(4), 263-278.

曲線架構法設計調和曲面

官大智* 李子才* 陳彥良* 莊榮宏**

*國立中山大學應用數學系

**國立交通大學資訊工程學系

摘 要

本文介紹一種數值方法—曲線架構法（wire-frame method）建構調和曲面。曲線的方程式由四次常微分方程式解得，亦即，將曲線模擬成受外力的彈性樑。四次常微分方程式由有限元素法求解，曲線解出之後，再用內差法分片地將調和曲面的方程式求出。